Supporting Information for

Highly efficient Ni-Mn/SiO_2 catalyst for the selective hydrogenation of biomass-derived levulinic acid to γ-valerolactone under mild conditions

Mengting Chen[a], Qifeng Zhong[a], Jiao Ma[a], Zhiyang Zhang[a], Yingxin Liu[a,c,*], Zuojun Wei[b,*], Shuguang Deng[c,*]

[a] College of Pharmaceutical Science, Zhejiang University of Technology, Hangzhou 310014, China

[b] Key Laboratory of Biomass Chemical Engineering of the Ministry of Education, College of Chemical and Biological Engineering, Zhejiang University, Hangzhou 310027, China

[c] School for Engineering of Matter, Transport and Energy, Arizona State University, 551 E. Tyler Mall, Tempe, AZ 85287, USA

* Corresponding authors

E-mail address: yxliu@zjut.edu.cn (Y.-X. Liu), weizuojun@zju.edu.cn (Z.-J. Wei), Shuguang.Deng@asu.edu (S.-G. Deng).

Experimental section

Catalyst characterization. Brunauer-Emmett-Teller (BET) surface areas of the catalysts were measured by pulsed N_2 adsorption-desorption method at -196 °C using Micromeritics ASAP 2460 analyzer. Prior to N_2 physisorption, the samples were degassed under vacuum at 250 °C for 3 h. H_2 temperature-programmed reduction (H_2-TPR) of the samples was performed on a FINESORB-3010 temperature programmed chemisorption instrument. About 100 mg of the dried catalyst samples were preheated at 150 °C under N_2 for 2 h, cooled to room temperature, and then reduced in the temperature range from room temperature to 900 °C at a heating rate of 10 °C·min^{-1} under a gaseous mixture of 10 vol% hydrogen in N_2. Hydrogen consumption was monitored on a thermal conductivity detector (TCD). Transmission electron microscopy (TEM) and high-angle annular dark-field scanning transmission electron microscope (HAADF-STEM) images were obtained using a Tecnai G2 F30 S-Twin instrument (FEI Co., USA) operated at an accelerating voltage of 300 kV. Particle size distribution of metal nanoparticles in each sample was determined from the corresponding TEM image by measuring the sizes of about 100 particles. X-ray photoelectron spectroscopy (XPS) spectra were obtained using an Escalab Mark II X-ray spectrometer (VG Co., United Kingdom) equipped with a magnesium anode (MgKα=1253.6 eV). Energy corrections were performed using a 1s peak of the pollutant carbon at 284.6 eV. The leaching of the catalysts was measured by using a PerkinElmer Optima 8000 spectrometer exploiting Inductively Coupled Plasma Optical Emission Spectrometry (ICP-OES). H_2 pulse chemisorption was performed using a Micromeritics ASAP 2020. Typically, 50 mg catalyst was loaded into a quartz U-tube reactor and reduced at 500 °C for 3 h. Subsequently, H_2 molecules were statically adsorbed at 35 °C. Ammonia temperature-programmed desorption analysis (NH_3-TPD) was performed on a chemisorption analyzer connected with a Hiden QIC-20 mass spectrometer analysis instrument (Hiden Analytical Ltd., United Kingdom). About 100 mg of

the dried sample was reduced at 500 °C for 3 h under a gaseous mixture of 10 vol% hydrogen in N_2, and then cooled down and swept with a gaseous mixture of 5 vol% NH_3 in N_2 at 50 °C for NH_3 adsorption. After adsorption equilibrium, the excess NH_3 was flushed at 50 °C with N_2 for 30 min. And then the sample was heated to 800 °C at a rate of 10 °C·min^{-1} and the signal of the outlet gas was recorded by TCD. The pyridine adsorbed FT-IR spectroscopy of the reduced sample was conducted on a Tensor 27 after the sample was well pressed into a wafer, followed by moving into the infrared quartz cell. The sample were additionally pre-treated for 2 h at 500 °C under a vacuum condition. Upon cooled to 120 °C, pyridine was flowed into the cell, while the spectra were recorded after pyridine was desorbed for 15 min at 50, 150 and 250 °C.

Table S1 Labels and calculated metal contents of catalysts

Catalyst Label	Ni (wt.%)	Mn (wt.%)	Ni/Mn (mol/mol)
Ni/SiO_2	2.0	0	N/A
$Ni\text{-}Mn(3:1)/SiO_2$	2.0	0.6	3
$Ni\text{-}Mn(2:1)/SiO_2$	2.0	0.9	2
$Ni\text{-}Mn(1:1)/SiO_2$	2.0	1.9	1
Mn/SiO_2	0	2.0	0

Table S2 Textural and structural properties of Ni/SiO_2 and $Ni\text{-}Mn(2:1)/SiO_2$

Sample	Surface area (m^2/g)[a]	Ni diameter (nm)[b]	Ni dispersion (%)[c]
SiO_2	287	/	/
Ni/SiO_2	192	3.61	0.67
$Ni\text{-}Mn(2:1)/SiO_2$	175	2.21	1.16

[a] Measured by nitrogen adsorption.

[b] Determined by TEM.

[c] Determined by H_2 chemisorption.

Table S3 XPS relative quantitative analysis of Ni/SiO_2 and $Ni\text{-}Mn(2:1)/SiO_2$ catalysts

Catalyst	Surface Ni (0)		Surface Ni (II)	
	B.E.[a] $2p_{3/2}/2p_{1/2}$ (eV)	Area (%)	B.E. $2p_{3/2}/2p_{1/2}$ (eV)	Area (%)
Ni/SiO_2	851.8/869.3	36.5	854.5/871.6	63.5
$Ni\text{-}Mn(2:1)/SiO_2$	852.1/869.5	37.8	854.8/871.9	62.2

[a] Abbreviation of binding energy.

Table S4 Acid property of Ni-Mn(2:1)/SiO_2 catalyst as calculated by FT-IR spectra

Temperature (°C)	W (mg)	Area of absorption peak		Amount of acid (μmol·g^{-1})			
		Assigned to Brønsted acid	Assigned to Lewis acid	Brønsted acid	Lewis acid	Total acid	B/L
50	19.2	0.024	1.069	1.0	33.4	34.4	0.03
150	19.2	0.013	0.847	0.5	26.5	27.0	0.02
250	19.2	0.008	0.306	0.3	9.5	9.9	0.03

Table S5 Catalytic performance of different Ni-based catalysts in hydrogenation of LA to GVL[a]

Entry	Catalyst	LA conv. (%)[b]	GVL yield (%)[b]
1	Ni/SiO_2	22.3	22.3
2	$Ni\text{-}V(1:1)/SiO_2$	4.0	4.0
3	$Ni\text{-}Zr(1:1)/SiO_2$	21.9	21.9
4	$Ni\text{-}Mn(1:1)/SiO_2$	64.7	64.7

[a]Reaction conditions: 4.3 mmol LA, 0.1 g catalyst, 10 mL 1,4-dioxane, 2 MPa H_2, 180 °C, 0.5 h. [b]Determined by gas chromatography equipped with a flame ionization detector (FID) using *n*-dodecane as an internal standard.

Table S6 Effect of different calcination temperatures on the performance of Ni-Mn(2:1)/SiO_2 for hydrogenation of LA to GVL[a]

Entry	Calcination temperature (°C)	LA conv. (%)[b]	GVL yield (%)[b]
1	No calcination	100	100
2	300	96.8	96.8
3	400	90.2	90.2
4	500	74.5	74.5

[a]Reaction conditions: 4.3 mmol LA, 0.1 g catalyst, 10 mL 1,4-dioxane, 2 MPa H_2, 180 °C, 2 h. [b]Determined by gas chromatography equipped with a flame ionization detector (FID) using *n*-dodecane as an internal standard.

Table S7 Effect of different solvents on hydrogenation of LA to GVL over Ni-Mn(2:1)/SiO_2[a]

Entry	Solvent	LA conv. (%)[b]	Sel. (%)[b]	
			GVL	HPA
1	1,4-Dioxane	100	100	/
2	Isopropanol	83.8	100	/
3	Tetrahydrofuran	100	97.3	2.7
4	Toluene	68.4	89.0	11.0
5	H_2O	/	/	/

[a]Reaction conditions: 4.3 mmol LA, 0.1 g catalyst, 10 mL solvent, 2 MPa H_2, 180 °C, 2 h.
[b]Determined by gas chromatography equipped with a flame ionization detector (FID) using *n*-dodecane as an internal standard.

Table S8 Hydrogenation of LA to GVL over various catalytic systems

Catalyst	H_2 pressure (MPa)	Temperature (^oC)	Time (h)	GVL Yield (%)	TOF[a] (h^{-1})	Ref.
7.9 wt.% Ni/Al_2O_3-CN-600	1	130	3	＞99	9.6	1
0.14 wt.% Ru/TiO_2@CN	6	30	13	100	277.7	2
1 wt.% $Co_{0.5}Re_{0.5}/TiO_2$	1.5	180	4	99.3	437	3
15%Ni-15%Co/Al_2O_3	3	110	3	99.5	3.6	4
Ni-Mo/C	10	200	2	100	2.5	5
43.1 wt.% $Ni_{0.58}$-$Sn_{0.42}$/AlOH	4	120	2	＞99	4.7	6
40 wt.% $Ni/MgAlO_{2.5}$	3	160	1	99.7	12.6	7
14.5 wt.% 2-Ni/C-400	4	160	3	94.5	5.2	8
Ni-MoO_x/C	0.8	140	5	97	19.4	9
6.3 wt.% Ni@NCMs-700	3	200	4	98	16.0	10
15 wt.% Ni/γ-Al_2O_3	5	200	4	92	11.0	11
2.0 wt.% Fe-Re(1:2)/TiO_2	4	180	4	95	57.7	12
20 wt.% Ni_3Fe NPs@C	2	130	2	89.6	17.6	13
40 wt.% Ni/Al_2O_3	3	180	2	99.2	10.2	14
Cu/ZrO_2-dp	3	150	5	＞99	5.5	15
26 wt.% CuPS-R_{350}-C_8-R_{350}	1.2	130	12	85.2	1.8	16
0.85 wt.% Ru/ZrO_2@C	1	140	2	99	495	17
34.4 wt.% Cu/ZrO_2-Al_2O_3	3	130	5	100	1.8	18
Ru/TiO_2-n	3	30	8	＞99	41.5	19
18.4 wt.% Cu/ZrO_2	3	200	5	100	3.4	20
2.0 wt.% Ru/FLG	4	20	12	99.7	365	21
82.4 wt.% Co/Al_2O_3	5	180	3	＞99	41.7	22
Cu-ZrO_2(1:1)	3.4	200	5	＞99.9	2.5	23
5 wt.% Pd/MCM-41	6	240	10	96.3	52.9	24
0.5 wt.% Ru-5 wt.% Ni/MMT	1.7	220	5	91	137.6	25
13.3 wt.% Ni-8.9 wt.% Cu/Al_2O_3	6.5	250	5	96	17.9	26
2 wt.% Ni-Mn(2:1)/SiO_2	2	180	2	100	190.2	This work
2 wt.% Ni-Mn(2:1)/SiO_2	2	140	5.5	100	27.0	This work

[a]Turnover frequency (TOF, h^{-1}) is defined as moles of target product formed/total moles of metal active sites per hour.

Table S9 Metal contents of Ni-Mn(2:1)/SiO_2 catalyst determined with ICP-OES.

Catalyst	Ni (wt.%)	Mn (wt.%)
Fresh Ni-Mn(2:1)/SiO_2	1.98	0.88
Reused Ni-Mn(2:1)/SiO_2	1.86	0.82

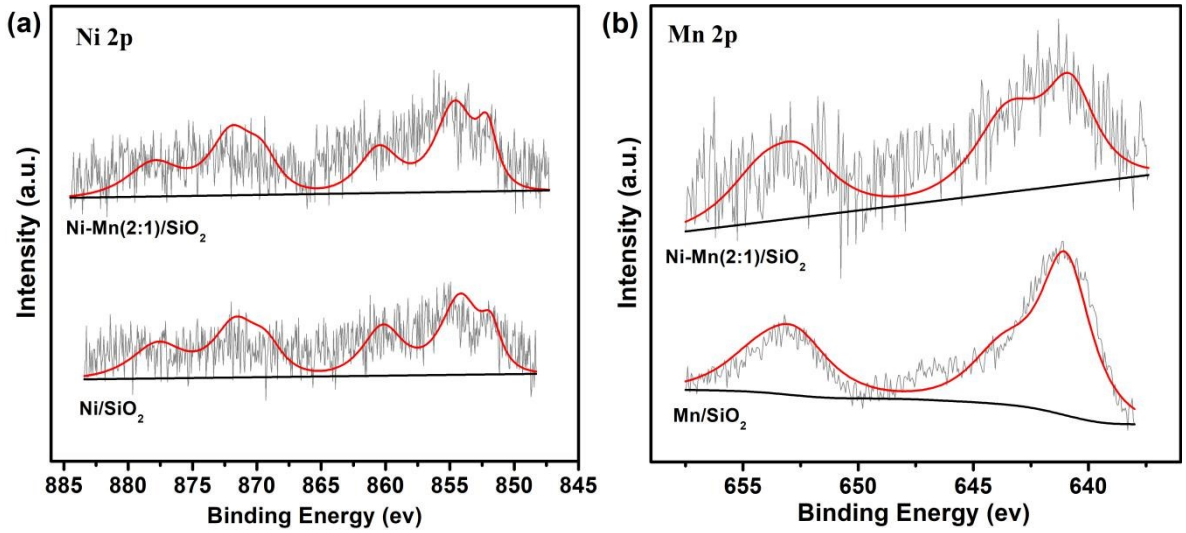

Fig. S1 The original XPS spectra of (a) Ni 2p and (b) Mn 2p of the reduced catalysts Ni/SiO_2, Mn/SiO_2 and $Ni\text{-}Mn(2:1)/SiO_2$.

References

1 L. Jiang, G.-Y. Xu and Y. Fu, *Green Chem.* 2021, **23**, 7065-7073.

2 K.-L. Zhang, Q.-L. Meng, H.-H. Wu, T.-Y. Yuan, S.-T. Han, J.-X. Zhai, B.-X. Zheng, C.-Y. Xu, W.-Wu, M.-Y. He and B.-X. Han, *Green Chem.* 2021, **23**, 1621-1627.

3 Z.-J. Wei, Q. Li, Y.-R. Cheng, M. Dong, Z.-Y. Zhang, X.-M. Zhu, Y.-X. Liu and Y. Sun, *ACS Sustainable Chem. Eng.* 2021, **9**, 10882-10891.

4 J. Bai, C.-W. Cheng, Y. Liu, C.-G. Wang, Y.-H. Liao, L.-G. Chen and L.-L. Ma, *Mol. Catal.* 2021, **516**, 112000.

5 B. P. Pinto, A. L. L. Fortuna, C. P. Cardoso and C. J. A. Mota, *Catal. Lett.* 2017, **147**, 751-757.

6 R. Rodiansono, M. D. Astuti, T. Hara, N. Ichikuni and S. Shimazu, *Catal. Sci. Technol.* 2016, **6**, 2955-2961.

7 K. Jiang, D. Sheng, Z.-H. Zhang, J. Fu, Z.-Y. Hou and X.-Y. Lu, *Catal. Today* 2016, **274**, 55-59.

8 S.-Q. Fang, Z.-B. Cui, Y.-T. Zhu, C.-G. Wang, J. Bai, X.-H. Zhang, Y.-Xu, Q.-Y. Liu, L.-G. Chen, Q. Zhang and L.-L. Ma, *J. Energy Chem.* 2019, **37**, 204-214.

9 K. Shimizu, S. Kanno and K. Kon, *Green Chem.* 2014, **16**, 3899-3903.

10 D.-W. Liu, L.-N. Zhang, W.-P. Han, M.-X. Tang, L.-G. Zhou, Y. Zhang, X.-K. Li, Z.-F. Qin and H.-Q. Yang, *Chem. Eng. J.* 2019, **369**, 386-393.

11 K. Hengst, M. Schubert, H. W. P. Carvalho, C.-B. Lu, W. Kleist and J. D. Grunwaldt, *Appl. Catal. A Gen.* 2015, **502**, 18-26.

12 X.-M. Huang, K.-T. Liu, W. L. Vrijburg, X.-H. Ouyang, A. I. Dugulan, Y.-X. Liu, M. W. G. M. T. Verhoeven, N. A. Kosinov, E. A. Pidko and E. J. M. Hensen, *Appl. Catal. B Environ.* 2020, **278**, 19314.

13 H.-J. Wang, C. Chen, H.-M. Zhang, G.-Z. Wang and H.-J. Zhao, *Chinese J. Catal.* 2018, **39**, 1599-1607.

14 J. Fu, D. Sheng and X.-Y. Lu, *Catalysts*, 2016, **6**, 6.

15 Z.-Y. Li, H.-G. Hao, J.-J. Lu, C.-M. Wu, R. Gao, J.-F. Li, C.-L. Liu and W.-S. Dong, *J Energy Chem*. 2021, **61**, 446-458.

16 Y.-J. Tsou, T.-D. To, Y.-C. Chiang, J.-F. Lee, R.-J. Kumar, P.-W. Chung and Y.-C. Lin,

ACS Appl. Mater. Interfaces, 2020, **12**, 54851-54861.

17 W.-X. Cao, W.-H. Luo, H.-G. Ge, Y. Su, A.-Q. Wang and T. Zhang, *Green Chem.* 2017, **19**, 2201-2211.

18 J.-F. Li, M.-J. Li, C.-X. Zhang, C.-L. Liu, R.-Z. Yang and W.-S. Dong, *J. Catal.* 2020, **381**, 163-174.

19 S.-P. Li, Y.-Y. Wang, Y.-D. Yang, B.-F. Chen, J. Tai, H.-Z. Liu and B.-X. Han, *Green Chem.* 2019, **21**, 770-774.

20 J.-F. Li, L. Zhao, J.-L. Li, M.-J. Li, C.-L. Liu, R.-Z. Yang and W.-S. Dong, *Appl Catal. A Gen.* 2019, **587**, 117244.

21 C.-X. Xiao, T. W. Goh, Z.-Y. Qi, S. N. Goes, K. Brashler, C. Perez and W.-Y. Huang, *ACS Catal.* 2016, **6**, 593-599.

22 X.-D. Long, P. Sun, Z.-L. Li, R. Lang, C.-G. Xia and F.-W. Li, *Chinese J. Catal.* 2015, **36**, 1512-1518.

23 A. M. Hengne and C. V. Rode, *Green Chem.* 2012, **14**, 1064-1072.

24 K. Yan, T. Lafleur, C. Jarvis and G.-S. Wu, *J. Clean. Prod.* 2014, **72**, 230-232.

25 G. B. Kasar, R. S. Medhekar, P. N. Bhosale and C. V. Rode, *Ind. Eng. Chem. Res.* 2019, **58**, 19803-19817.

26 I. Obregón, E. Corro, U. Izquierdo, J. Requies and P. L. Arias, *Chinese J. Catal.* 2014, **35**, 656-662.